

07,13

Low-temperature heat capacity of the Ni–Mn–In Heusler alloys

© L.N. Khanov¹, A.T. Kadirbardeev¹, A.V. Mashirov², A.M. Aliev¹

¹ Amirkhanov Institute of Physics, Daghestan Federal Research Center, Russian Academy of Sciences, Makhachkala, Russia

² Kotelnikov Institute of Radio Engineering and Electronics, Russian Academy of Sciences, Moscow, Russia

E-mail: hanov82@mail.ru

Received July 17, 2025

Revised July 17, 2025

Accepted July 19, 2025

This paper presents the results of an experimental study of the magnetization (M) and heat capacity (C_P) of polycrystalline samples $\text{Ni}_{49.3}\text{Mn}_{40.4}\text{In}_{10.3}$, $\text{Ni}_{45.48}\text{Mn}_{40.52}\text{In}_{14}$, $\text{Ni}_{46.78}\text{Mn}_{38.42}\text{In}_{14.8}$, $\text{Ni}_{41}\text{Mn}_{40.5}\text{In}_{18.5}$ of the Heusler alloys in the temperature range of 4–350 K. The obtained curves exhibit anomalies corresponding to magnetostructural (if any) and magnetic phase transitions. From the analysis of the low-temperature dependence of the heat capacity, the electron contributions to the heat capacity, the Debye temperatures (θ_D) and the density of electron states at the Fermi level of the studied samples were obtained. It was found that the Debye temperature (301–384 K) is an increasing function of e/a .

Keywords: Heusler alloys, helium temperatures, Debye temperature, phase transitions, magnetization.

DOI: 10.61011/PSS.2025.08.62266.201-25

1. Introduction

In recent years, due to global problems of energy consumption and reduction of emissions of harmful substances during operation of gas refrigerators, intense studies are dedicated to magnetic compounds, in which a gigantic value of the magnetocaloric effect (MCE) is observed near the room temperatures [1]. One of these compounds is Ni–Mn–X Heusler alloys (X = Ga, Sn, Sb, In). The Ni–Mn-based alloys demonstrate the gigantic MCE [2–5], an elastocaloric effect [6], a shape memory effect [7], superelasticity [3,8] and gigantic magnetoresistance [9,10]. It is important to study the Ni–Mn-based alloys due to presence of anomalous magnetic and structural properties, since the magnetostructural phase transition is almost always accompanied by pronounced changes of the physical properties of the alloys [11]. The paramagnetic–ferromagnetic phase transition exhibits the direct MCE near T_C . The ferromagnetic–antiferromagnetic phase transition exhibits the reverse MCE. The reverse MCE in volumetric samples of the Heusler alloys is studied in the papers [4,5,12,13]. A number of interesting physical effects is observed near the magnetostructural phase transition (MSPT).

For practical application of the magnetocaloric materials in a magnetic cooling technology, it is necessary to take into account not only the magnetocaloric properties, but other physical parameters as well. For example, heat capacity plays a key role, since it determines an amount of heat absorbed or release by the material during temperature variation. A study of heat capacity can provide information about a nature and specific features of the phase transitions, electron and magnon contributions to total heat capacity. MCE is indirectly calculated using data of heat capacity

measurements. Evaluation of the contributions by the various subsystems to total heat capacity, determination of a Debye temperature, etc. requires measurements of heat capacity within a wide temperature range, including a range of the helium temperatures. Low-temperature heat capacity of the Heusler alloys can be studied for understanding their thermodynamic properties and behavior at the various temperature modes.

The present paper provides results of the experimental study of magnetization (M) and heat capacity (C_P) of the Heusler alloy polycrystalline samples $\text{Ni}_{49.3}\text{Mn}_{40.4}\text{In}_{10.3}$, $\text{Ni}_{45.4}\text{Mn}_{40.52}\text{In}_{14}$, $\text{Ni}_{46.78}\text{Mn}_{38.42}\text{In}_{14.8}$, $\text{Ni}_{41}\text{Mn}_{40.5}\text{In}_{18.5}$ within the wide temperature range, including the helium temperatures (4.2 K).

2. Samples and experimental procedure

The samples for the study were produced by argon atmosphere arc melting with three turns and four melt-downs. Then homogenizing annealing at $T = 900$ °C during 48 h in vacuum was performed. The elemental chemical composition of the annealed samples was determined using energy-dispersive X-ray spectroscopy (EDX).

Magnetization was measured in an automatic mode within the temperature range 50–400 K in the magnetic fields of 50 Oe by an installation Quantum Design PPMS-9T. The sizes of the studies samples were $2 \times 2 \times 1$ mm, a weight of each was about 50 mg. The measurements were performed in three modes: zero-field cooling with subsequent measurements in a certain magnetic field in the heating mode (ZFC), cooling in the magnetic field (FC) and heating in the magnetic field (FH). The heating and cooling

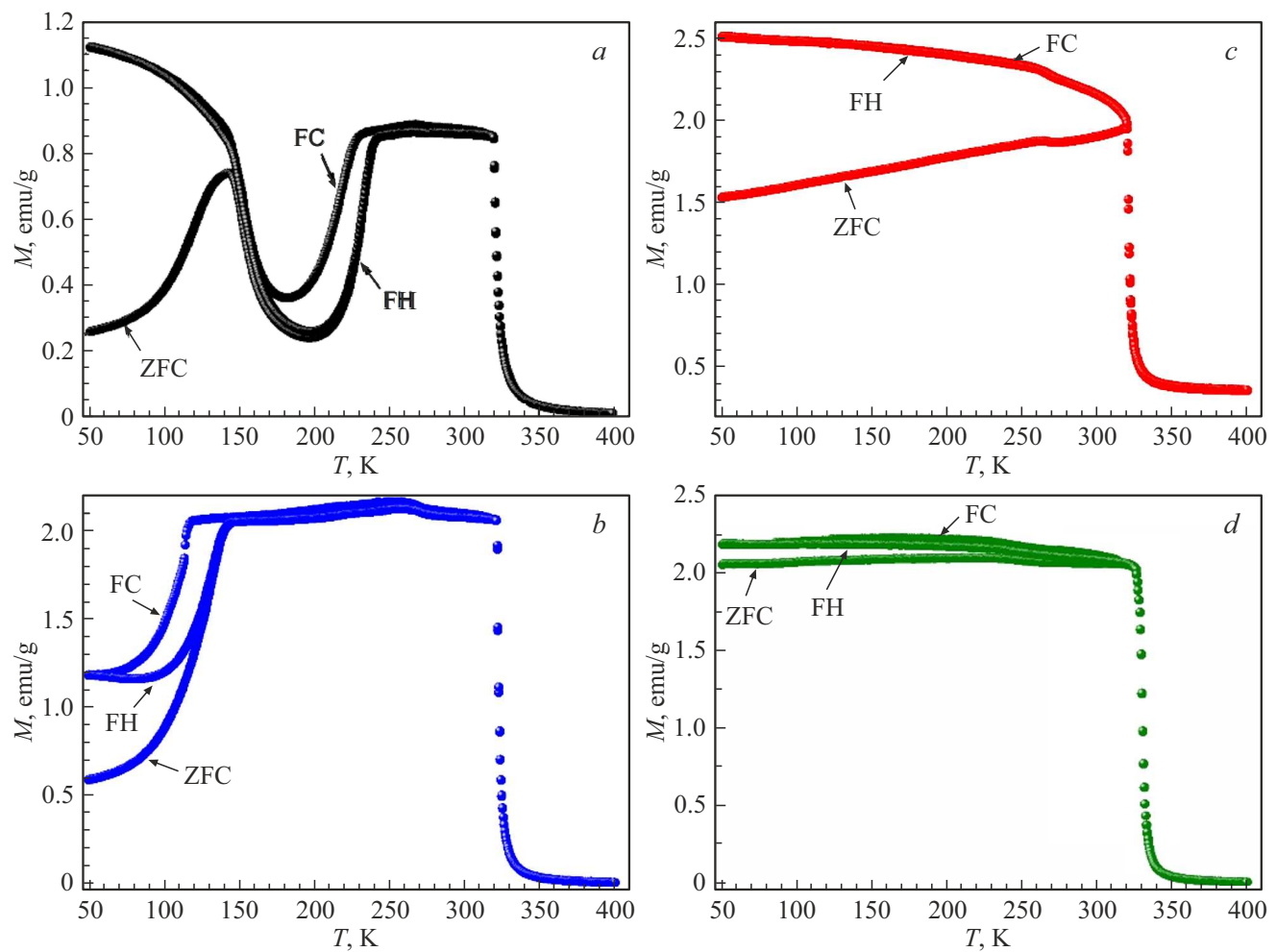


Figure 1. Temperature dependence of magnetization of the Ni–Mn–In alloys in the magnetic field of 50 Oe. *a*) Ni_{49.3}Mn_{40.4}In_{10.3}; *b*) Ni_{45.48}Mn_{40.52}In₁₄; *c*) Ni_{46.78}Mn_{38.42}In_{14.8}; *d*) Ni₄₁Mn_{40.5}In_{18.5}.

rate was 2 K/min. Heat capacity (C_P) was measured by a modulation calorimetry method (AC-calorimetry). The studies were carried out within the temperature range 4.2–350 K. The helium temperatures (4.2 K) were obtained by means of a close-cycle cryostat CFSG-310 with a sample in the exchange gas. The temperature variation rate was 0.3 K/min within the phase transitions and within the helium temperatures and 1 K/min within the remaining temperature range.

3. Results and discussion

Figure 1 shows curves of the temperature dependence of magnetization of the Heusler polycrystalline alloys Ni_{49.3}Mn_{40.4}In_{10.3}, Ni_{45.48}Mn_{40.52}In₁₄, Ni_{46.78}Mn_{38.42}In_{14.8}, Ni₄₁Mn_{40.5}In_{18.5}, which are obtained in the magnetic field of 50 Oe. The thermomagnetic measurements of $M(T)$ were carried out by a protocol: heating after zero-field cooling (ZFC), field cooling (FC) and field heating (FH). All the four alloys within the range $T = 310$ – 330 K in the cooling

mode exhibit magnetic anomalies as a sharp increase of magnetization, which is related to a transition of austenite from a paramagnetic state into a ferromagnetic state.

The alloys Ni_{49.3}Mn_{40.4}In_{10.3}, Ni_{45.48}Mn_{40.52}In₁₄ within the range $T = 100$ – 250 K exhibit the magnetostructural phase transition (martensite–austenite) with a temperature hysteresis, which is typical for the I-order phase transition (Figure 1, *a, b*). A pronounced hysteresis can indicate structural changes that accompany this transition [14–16]. This transition is not observed for the alloys Ni_{46.78}Mn_{38.42}In_{14.8}, Ni₄₁Mn_{40.5}In_{18.5}. I.e., down to the low temperatures (50 K), the main state is ferromagnetic austenite. The similar pattern is observed in the alloys Ni₅₀Mn_{50–x}In_x ($x < 10$) [17] and Ni₅₀Mn_{50–x}Sb_x ($x \geq 17$) [18].

Figure 2 shows the experimental curves of the temperature dependence of heat capacity of the Heusler polycrystalline alloys Ni_{49.3}Mn_{40.4}In_{10.3}, Ni_{45.48}Mn_{40.52}In₁₄, Ni_{46.78}Mn_{38.42}In_{14.8}, Ni₄₁Mn_{40.5}In_{18.5} in the zero magnetic field in the heating mode. For clarity, the curves $C_P(T)$ are shifted by 50 J/mol · K, 100 J/mol · K and 150 J/mol · K relative to the lowest one (the black circles).

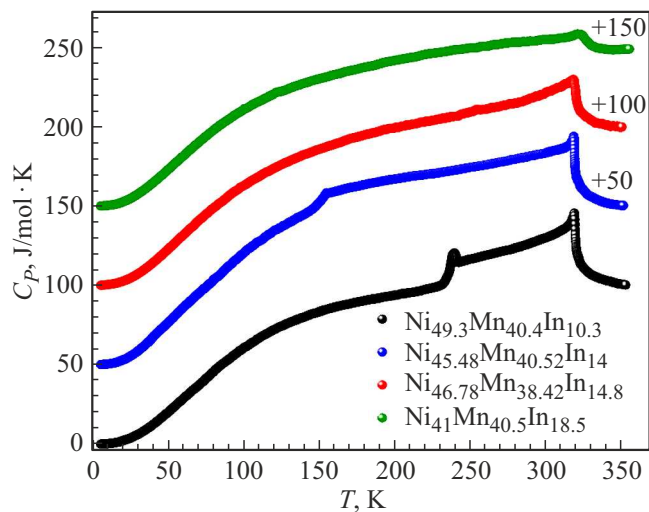


Figure 2. Temperature dependence of heat capacity of the Heusler alloys in the zero magnetic field in the heating mode. For clarity, the curves are shifted by 50 J/mol·K, 100 J/mol·K and 150 J/mol·K relative to the lowest one (the black circles).

Within the high-temperature range ($T = 310$ –330 K), the obtained curves exhibit clearly pronounced anomalies as a λ -peak, which are typical for these alloys and correspond to the ferromagnetic–paramagnetic phase transition (the magnetic transition) that occurs in the austenite phase. The heat capacity peak exists due to energy consumption during the phase transition, which is spent for orientational disordering of the magnetic moments around T_C . A nature of the magnetic transition in the Heusler alloys is described by us in more detail in the studies[16,19]. The alloys $\text{Ni}_{49.3}\text{Mn}_{40.4}\text{In}_{10.3}$, $\text{Ni}_{45.48}\text{Mn}_{40.52}\text{In}_{14}$ at the temperatures 239 K and 155 K exhibit the second anomaly that corresponds to the MSPT (antiferromagnetic–ferromagnetic). As can be seen from Figure 2, the heat capacity curves correlate with the magnetization behavior (Figure 1).

A particular interest in the heat capacity curve is paid to the low-temperature range (4–20 K). Measurement of low-temperature heat capacity is an important tool, which is usually used for empirically evaluating a heat capacity electron coefficient γ and the Debye temperature θ_D .

Specific heat capacity of a magnetic solid body is formed by electrons, lattice vibrations (phonons) and spin excitations (magnons). Within the low-temperature range, the phonon contribution to molar specific heat capacity is approximately equal to a Debye term

$$C_D(T) \approx \beta T^3, \quad (1)$$

which is related to the Debye temperature (θ_D) by an expression

$$\theta_D = \left(\frac{12\pi^4 R}{5\beta} \right)^{1/3}, \quad (2)$$

where R — the universal gas constant, β — the coefficient of a phonon component of heat capacity.

The magnon (magnetic) contribution to heat capacity of the solid body is

$$C_M(T) = \alpha T^{3/2}. \quad (3)$$

The temperature-independent coefficient α is reversely proportional to the third power of the Curie temperature and is not related to the Debye temperature [20,21].

The contribution by the electron component to total heat capacity is of a linear nature and can be described by a formula:

$$C_{El}(T) = \gamma T. \quad (4)$$

Therefore, total heat capacity of the solid body satisfies the equation

$$C = \gamma T + \alpha T^{3/2} + \beta T^3. \quad (5)$$

Figure 3, *a* shows experimentally-obtained curves of heat capacity for the four Ni–Mn–In alloys within the low temperatures (4–20 K) in the zero magnetic field in the heating mode. Authors of the paper [22] have carried out studies for determining a magnetic part of heat capacity of the $\text{Ni}_{50}\text{Mn}_{50-x}\text{In}_x$ nonstoichiometric alloy ($x = 13, 16.2$) and shown that if an initial fragment of the heat capacity curve is linear, then the magnetic contribution is negligible and it can be omitted in the formula (5). Otherwise, the magnetic part of heat capacity can be compared in magnitude with the nonmagnetic part. Since for our studied alloys the low-temperature part of heat capacity is of a linear nature (Figure 3, *b*), then the magnetic contribution is not taken into account and the (5) can be written as follows

$$C = \gamma T + \beta T^3. \quad (6)$$

The expressions (6) were used to obtain the low-temperature data for heat capacity (the dotted lines in Figure 3, *b*). The coefficient γ, β for the studied materials were selected so that the approximation curve coincides with the measured data on the graph of C_P/T on T^2 (Figure 3, *b*). By extrapolating straight portions of the dependences C_P/T on T^2 (shown in Figure 3, *b*) to $T = 0$, we have estimated values of specific electron heat capacity γ for the four studied Ni–Mn–In alloys. Using a cubic term of the formula (6), which is caused by the phonon contributions, and the expression (2), it is possible to determine the Debye temperature (θ_D) for each composition.

The linear term (γ) is proportional to the density of states at the Fermi level by the relationship:

$$N(E_F) = \frac{3\gamma}{\pi^2 k_B^2}, \quad (7)$$

where k_B — the Boltzmann constant.

This expression was used to determined the densities of state at the Fermi levels for the studied materials.

The low-temperature range of heat capacity of the polycrystalline alloys $\text{Ni}_{49.3}\text{Mn}_{40.4}\text{In}_{10.3}$, $\text{Ni}_{45.48}\text{Mn}_{40.52}\text{In}_{14}$, $\text{Ni}_{46.78}\text{Mn}_{38.42}\text{In}_{14.8}$, $\text{Ni}_{41}\text{Mn}_{40.5}\text{In}_{18.5}$ was analyzed to determine the characteristic parameters γ, β , the typical Debye

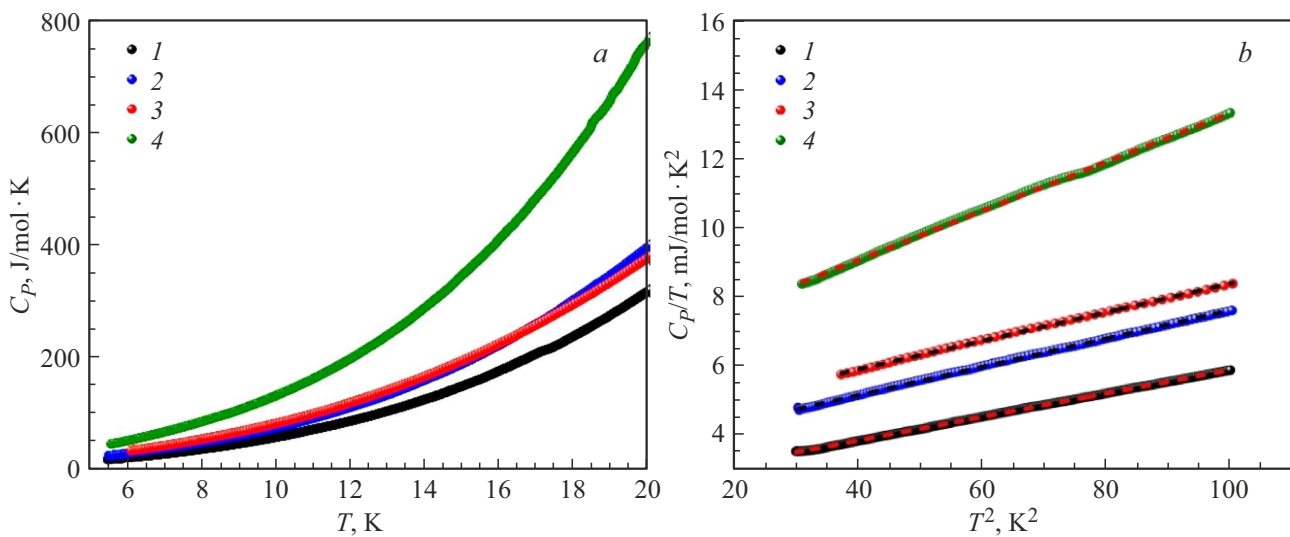


Figure 3. *a)* Low-temperature heat capacity for the compositions: 1 — $\text{Ni}_{49.3}\text{Mn}_{40.4}\text{In}_{10.3}$, 2 — $\text{Ni}_{45.48}\text{Mn}_{40.52}\text{In}_{14}$, 3 — $\text{Ni}_{46.78}\text{Mn}_{38.42}\text{In}_{14.8}$, 4 — $\text{Ni}_{41}\text{Mn}_{40.5}\text{In}_{18.5}$; *b)* the dependence of C_p/T on T^2 for the same samples is shown by the solid lines and the dotted lines mark approximation by the formula (6).

Values of the coefficients of low-temperature heat capacity and some characteristics of the Heusler alloys

	$\text{Ni}_{49.3}\text{Mn}_{40.4}\text{In}_{10.3}$	$\text{Ni}_{45.48}\text{Mn}_{40.52}\text{In}_{14}$	$\text{Ni}_{46.78}\text{Mn}_{38.42}\text{In}_{14.8}$	$\text{Ni}_{41}\text{Mn}_{40.5}\text{In}_{18.5}$
γ ($\text{mJ/mol} \cdot \text{K}^2$)	2.51	3.55	4.28	6.28
β ($\text{mJ/mol} \cdot \text{K}^4$)	0.034	0.041	0.0414	0.071
$N(E_F)$ ($1/\text{eV} \cdot \text{mol}$)	$6.43 \cdot 10^{23}$	$9.1 \cdot 10^{23}$	$1.1 \cdot 10^{24}$	$1.61 \cdot 10^{24}$
θ_D (K)	384	361	360	301
e/a	8.07	7.8	7.81	7.49

temperatures (θ_D), the densities of states at the Fermi level ($N(E_F)$), which are tabularized.

Since concentrations of the three elements (Ni, Mn and In) are simultaneously changed in the studied alloys, then electron-per-atom ratios (e/a) are calculated by the formula (8) in order to compare the characteristic parameters and the Debye temperature. The calculation results are shown in the table. Here, the number of valence electron per atom for Ni, Mn and In is 10, 7 and 3, respectively. A portion of the atomic weight is written as at.%

$$e/a = (10 \cdot (\text{Ni at.}\%) + 7 \cdot (\text{Mn at.}\%) + 3 \cdot (\text{In at.}\%)) / 100. \quad (8)$$

The Figure 4 shows dependences of the heat capacity electron coefficient and the Debye temperature on the number of electrons per atoms for the studied alloys $\text{Ni}_{49.3}\text{Mn}_{40.4}\text{In}_{10.3}$, $\text{Ni}_{45.48}\text{Mn}_{40.52}\text{In}_{14}$, $\text{Ni}_{46.78}\text{Mn}_{38.42}\text{In}_{14.8}$, $\text{Ni}_{41}\text{Mn}_{40.5}\text{In}_{18.5}$ (the filled blue and red circles) as well as for $\text{Ni}_{50}\text{Mn}_{50-x}\text{In}_x$ ($x = 3, 5, 8, 10, 13, 15$) (the filled blue and red squares) and $\text{Ni}_{50}\text{Mn}_{50}$ (the unfilled circles), whose values are taken from the studies [17,23].

In his studies [17,23], Umetsu has investigated the Ni–Mn–In alloy at the low temperatures (2–80 K) within

the range of the concentrations of the valence electrons (e/a) from 7.9 to 8.5. In our study, we have considered these alloys within the e/a range from 7.49 to 8.07. Our studies of the heat capacity electron coefficient and the Debye temperatures continue the Umetsu studies. It can be seen from Figure 4 that our obtained values of γ coincide with the linear curve: with increase of the number of electrons per atom the electron contribution to heat capacity decreases. The values obtained by us for θ_D well correlate with data of the authors of the papers [17,23]. The values of the Debye temperature linearly increase with the increase of the number of electron per atom. Small differences in absolute values of θ_D are most likely related to specific features of an alloy production technology.

It was reported in the study [24] that for the $\text{Ni}_{50}\text{Mn}_{50-x}\text{In}_x$ alloy the crystal structure varies from the tetragonal type $\text{L}1_0$ when $x = 0$ to the monoclinic multilayer structure with the increase of the In content. The magnetic properties are a collinear antiferromagnetic with the high Néel temperature when $x = 0$ [25]. This properties changes to complex magnetic properties, which have no long-range magnetic order and exhibit a blocking behavior [24,26]. Since when varying the In content,

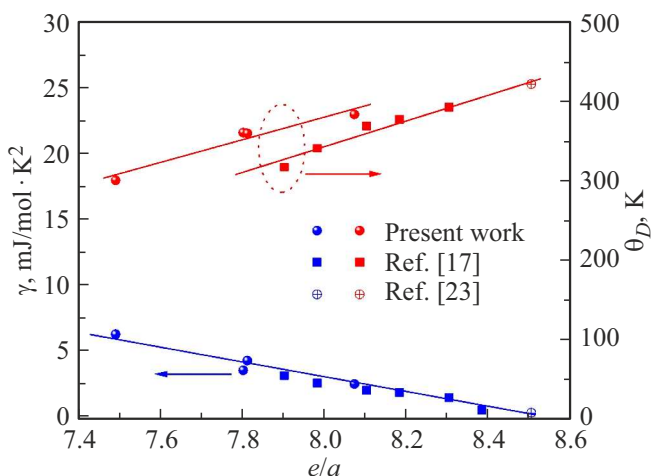


Figure 4. Dependences of the heat capacity electron coefficient (γ) and the Debye temperature (θ_D) on electrons per atom (e/a). The filled blue and red circles are for the studied alloys. The filled blue and red squares are for $\text{Ni}_{50}\text{Mn}_{50-x}\text{In}_x$ ($x = 3, 5, 8, 10, 13, 15$). The unfilled circles are for $\text{Ni}_{50}\text{Mn}_{50}$. The lines are given for eye orientation.

no sharp changes of either the crystal structure or the magnetic properties are observed, the increase of the Debye temperature can be induced by an effect of substitution of the heavy element of indium. The decrease of γ with the increase of the number of electrons per atom can be related to a loss of antiferromagnetic stability.

4. Conclusion

Thus, we have studied magnetization and heat capacity of the Heusler alloy polycrystalline samples $\text{Ni}_{49.3}\text{Mn}_{40.4}\text{In}_{10.3}$, $\text{Ni}_{45.48}\text{Mn}_{40.52}\text{In}_{14}$, $\text{Ni}_{46.78}\text{Mn}_{38.42}\text{In}_{14.8}$, $\text{Ni}_{41}\text{Mn}_{40.5}\text{In}_{18.5}$ within the wide temperature range from 4 to 350 K. The obtained curves exhibit anomalies that correspond to the magnetostructural (if available) and magnetic phase transitions. The heat capacity curves correlate with the magnetization behavior. The main purpose of this study was analysis of the low-temperature range of heat capacity of the Ni–Mn–In Heusler alloys and using the curve C_P/T on T^2 to determine the characteristic parameters (γ, β), the typical Debye temperature (θ_D) and the density of states at the Fermi level ($N(E_F)$). The obtained values of the electron contribution of the Debye temperature agree with the literature data.

Funding

This study was carried out under state assignment No. FFUU-2025-0043.

Conflict of interest

The authors declare that they have no conflict of interest.

References

- [1] K.A. Gschneidner Jr., V.K. Pecharsky, A.O. Tsokol. *Rep. Prog. Phys.* **68**, 1479 (2005).
- [2] R. Kainuma, Y. Imano, W. Ito, Y. Sutou, H. Morito, S. Okamoto, K. Ishida. *Nature* **439**, 957 (2006).
- [3] T. Krenke, E. Duman, M. Acet, E.F. Wassermann, X. Moya, L. Manosa, B. Ouladdiaf. *Phys. Rev. B* **75**, 104414 (2007).
- [4] A. Planes, L. Manosa, M. Acet, J. Phys.: Condens. Matter **21**, 233201 (2009).
- [5] A.K. Pathak, I. Dubenko, J.C. Mabon, Sh. Stadler, N. Ali, *J. Phys. D* **42**, 045004 (2009).
- [6] Y.J. Huang, Q.D. Hu, N.M. Bruno, J.H. Chen, I. Karaman, J.H. Ross Jr, J.G. Li. *Scr. Mater.* **105**, 42 (2015).
- [7] R. Kainuma, Y. Imano, W. Ito, H. Morito, Y. Sutou, K. Oikawa, T. Kanomata. *Appl. Phys. Lett.* **88**, 192513 (2006).
- [8] V.A. Chernenko, V. L'vov, J. Pons, E. Cesari. *J. Appl. Phys.* **93**, 2394 (2003).
- [9] K. Koyama, H. Okada, K. Watanabe, T. Kanomata, R. Kainuma, W. Ito, K. Ishida. *Appl. Phys. Lett.* **89**, 182510 (2006).
- [10] S.Y. Yu, L. Ma, G.D. Liu, Z.H. Liu, J.L. Chen, Z.X. Cao, X.X. Zhang. *Appl. Phys. Lett.* **90**, 242501 (2007).
- [11] T. Graf, C. Felser, S. Parkin. *Progress in solid state chemistry* **39**, 1–50 (2011).
- [12] T. Krenke, E. Duman, M. Acet, E.F. Wassermann, X. Moya, L. Manosa, A. Planes. *Nature Mater.* **4**, 450 (2005).
- [13] V.V. Khovaylo, K.P. Skokov, O. Gutfleisch, H. Miki, T. Takagi, T. Kanomata, V.V. Koledov, V.G. Shavrov, G. Wang, E. Palacios, J. Bartolomé, R. Burriel. *Phys. Rev. B* **81**, 214406 (2010).
- [14] V. Recarte, J.I. Perez-Landazabal, V. Sanchez-Alarcos, J.A. Rodríguez-Velamazan. *Acta Materialia* **60**, 1937 (2012).
- [15] L.N. Khanov, A.B. Batdalov, A.V. Mashirov, A.P. Kamantsev, A.M. Aliev. *Fizika tverdogo tela* **60**, 1099 (2018). (in Russian).
- [16] A.B. Batdalov, A.M. Aliev, L.N. Khanov, V.D. Butchelnikov, V.V. Sokolonsky, V.V. Koledov, V.G. Shavrov, A.V. Mashirov, E.T. Dilmieva. *ZhETF* **149**, 1011 (2016). (in Russian).
- [17] R.Y. Umetsu, X. Xu, W. Ito, R. Kainuma. *Metals* **7**, 414 (2017).
- [18] A. Kosogor, R.Y. Umetsu, V. Golub, X. Xu, R. Kainuma. *Journal of Alloys and Compounds* **988**, 174130 (2024).
- [19] A.B. Batdalov, L.N. Khanov, A.V. Mashirov, V.V. Koledov, A.M. Aliev. *Journal of Applied Physics* **129**, 123901 (2021).
- [20] A.B. Batdalov, L.N. Khanov, A.A. Mukhuchev, A.V. Mashirov, A.M. Aliev. *Fizika tverdogo tela* **66** (10), 1805 (2024). (in Russian).
- [21] A.I. Akhiezer, V.G. Bar'yakhtar, S.V. Peletinskii. *Spin waves*. Translated [from the Russian] by S. Chomet. Amsterdam, North-Holland Pub. Co., 1968. North-Holland series in low temperature physics, v. 1.
- [22] S.V. Vonsovskij, *Magnetism* (Vol. 22053) Wiley (1974).
- [23] R.Y. Umetsu, A. Sakuma, K. Fukamichi. *Met. Mater. Process.* **15**, 67–94 (2003).
- [24] T. Krenke, M. Acet, E.F. Wassermann, X. Moya, L. Manosa, A. Planes. *Phys. Rev. B* **73**, 174413 (2006).
- [25] L. Pal, E. Kren, G. Kadar, P. Szabo, T. Tarnoczi. *J. Appl. Phys.* **39**, 538–544 (1968).
- [26] V.V. Khovaylo, T. Kanomata, T. Tanaka, M. Nakashima, Y. Amako, R. Kainuma, R.Y. Umetsu, H. Morito, H. Miki. *Phys. Rev. B* **80**, 144409 (2009).

Translated by M. Shevelev